A Novel Differential Fed High Gain Patch Antenna Using Resonant Slot Loading

Zubair AHMED [1], *Muhammad Mansoor AHMED* [1], *Mojeeb Bin IHSAN* [2]

[1] Dept. of Electrical Engineering, Capital University of Science and Technology, Islamabad, Pakistan
[2] Dept. of Electrical Engineering, National University of Sciences and Technology, Islamabad, Pakistan

zubair.ahmed@ee.ceme.edu.pk, mansoor@cust.edu.pk, mojeeb-eme@nust.edu.pk

Submitted December 26, 2017 / Accepted May 26, 2018

Abstract. *Inspired by slotted waveguide antennas, a pair of resonant slots is placed in the center out of phase region of TM_{30} mode rectangular patch antenna which acts as a new radiating edge. Superposition of radiated fields of TM_{30} mode patch and fundamental mode of slots results in high directivity radiator with reduced side lobe levels (SLL). It is shown that by making the resonant frequencies of patch and slots equal, good impedance matching and gain flatness can be achieved. The placement of resonant slots also has a slight adverse affect on the in phase current distribution resulting in asymmetric radiation pattern. It is demonstrated that a differential feeding scheme can be employed to achieve gain enhancement and symmetric radiation pattern by keeping the desired in phase current distribution intact. The proposed differential fed slot loaded patch antenna has symmetric radiation pattern with reduced cross polarization levels. It shows a measured gain of 12.8 dBi, SLL of –12 dB and $S_{11} \leq -10$ dB impedance bandwidth of 21 MHz. The proposed antenna can be used as a substitute for 2 × 2 array of patch antennas operating in fundamental mode and is suitable for integration with differential circuits.*

Keywords

Higher order mode, differential fed, slot loading, high gain, low side lobe level, microstrip antenna

1. Introduction

High directivity planar antennas with low side lobe levels (SLL) are desired in various wireless communication applications. Patch antennas operating in fundamental mode have low gain typically 5–8 dBi [1]. Although, higher order mode operation in patch antennas can be used to increase directivity due to increase in size but high E-plane SLL limits their use for most practical applications.

Recently, there is a renewed interest to improve the radiation characteristics of higher order mode patch antennas [2–6]. A dual mode circular patch antenna was proposed in [2] wherein superposition of radiated field was used to achieve gain enhancement and SLL reduction by employing simultaneous excitation of TM_{11} and TM_{13} modes in a stacked configuration. However, due to multilayer nature, antenna has complex geometry and is difficult to fabricate. A differential fed shorted TM_{30} mode rectangular patch is presented in [3] which has no E-plane SLL but resulting antenna has low gain and fabrication cost increases due to presence of via. In [4], E-plane SLL of TM_{12} mode circular patch antenna was reduced by employing a high dielectric constant substrate. However, surface wave losses in high dielectric substrates can cause ripple in main beam and reduction in antenna efficiency.

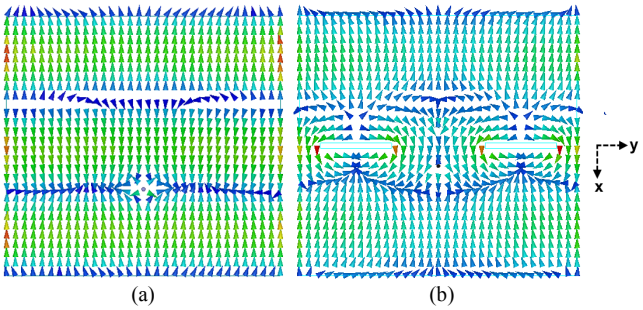

Fig. 1. Simulated surface current distribution: (a) Conventional TM_{30} mode patch antenna. (b) Proposed antenna.

In the past, slot loading has been employed to improve the impedance bandwidth or SLL reduction in higher order mode patch antenna. U, E and C slots [7–10] can be used to achieve wide impedance bandwidth in patch antennas by coupling the different resonant frequencies. Although, extensive literature can be found to improve impedance bandwidth using slot loading. Very few references are available for radiation pattern shaping using slot loading approach. The main cause of high SLL in higher mode patch antenna is out of phase surface current distribution as shown in Fig. 1(a). In [11], a reactive slot loading was employed to make higher order TM_{30} mode current distribution similar to fundamental TM_{10} mode. As a result SLL are eliminated but at the expense of reduction in antenna directivity. A non resonant slot loading was used in [6] to reduce the SLL of TM_{12} mode circular patch antenna. However, antenna has asymmetric radiation pattern and high cross polarization levels.

In this paper we propose a resonant slot loading technique and differential feeding to achieve high gain, low SLL single layer patch antenna with symmetric radiation pattern and low cross polarization. The method employs a linear 1 × 2 array of slots which perturbs the out of phase current distribution in TM_{30} mode patch to create additional in phase radiators. It is shown that by perturbing only out of phase higher mode current distribution while keeping in phase current distribution intact, both directivity enhancement and SLL reduction can be achieved simultaneously. The slot loading technique presented here is different in the sense that it is used to improve the radiation characteristics of patch rather than impedance bandwidth enhancement. Moreover, in the proposed technique instead of removing the out of phase surface current distribution, it has been utilized to achieve performance enhancement of antenna. Different parameters that influence the performance of antenna are investigated. It is shown that by making the resonant frequency of patch and slots equal, good impedance matching and gain flatness can be achieved. It is worthwhile to mention that differential feeding is usually employed to suppress cross-polarization [12] or to achieve symmetric radiation pattern [3] whereas current work demonstrates that differential feeding can also be used to increase directivity. A peak directivity of 13.3 dB is achieved by means of proposed resonant slot loading and differential feeding technique with good SLL of –12.7 dB. To the best of our knowledge this is the highest reported peak directivity for TM_{30} mode patch antenna in single layer configuration using Teflon based substrate. In the past, fractal antennas operating in higher order fracton or fractino mode showed higher directivity [13] compared to their Euclidian counterpart. The proposed antenna demonstrates a practical realization of high directivity patch antenna employing simple Euclidian geometry and larger directivity compared to fractal antennas.

2. Antenna Geometry and Radiation Mechanism

The proposed antenna geometry is shown in Fig. 2. The antenna is designed to operate at resonant frequency of 3 GHz. Arlon CuClad substrate having $\varepsilon_r = 2.2$ and thickness $h = 1.524$ mm was used for antenna design. The rectangular patch has length L and width W. A pair of slots, each having length ℓ and width t is cut at the center of patch parallel to the radiating edges. The distance between the centers of slots is d. The antenna is fed using two differential probes symmetrically located around the center and a distance F apart.

The working of the antenna can be explained by taking an analogy with slotted waveguide antenna. In a waveguide, radiating slot can be created by placing a resonant slot such that surface current lines are interrupted [14]. Simulated surface current distribution of conventional TM_{30} mode patch is shown in Fig. 1(a). It consists of two

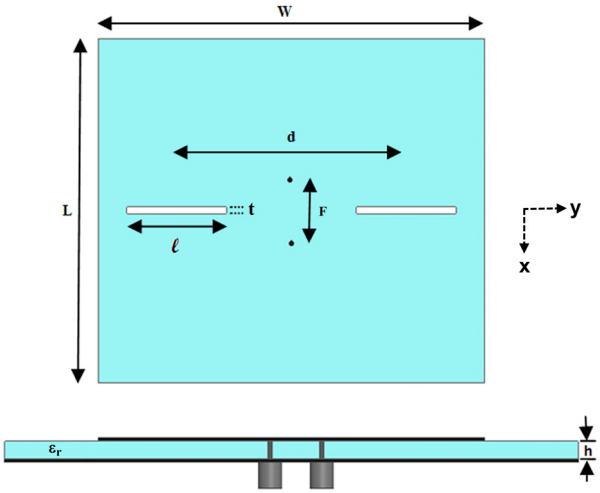

Fig. 2. Geometry of the proposed antenna ($W = 10.1$, $L = 9$, $\ell = 2.6$, $d = 6$, $t = 0.18$, $F = 2$, all dimensions in cm).

in phase regions located along the radiating edges and a center out of phase undesired region. By placing half wave length slots in the center region, slots can be excited in their fundamental mode as shown in Fig. 1(b). Use of differential feeding ensures the symmetric surface current distribution on the patch. The slots placed in the center portion of the patch interrupt the out of phase current distribution such that the induced slot field is in phase and polarization matched with the aperture field associated with the radiating edges of the TM_{30} mode patch. It is worthwhile to mention that a single higher order mode slot cannot be used in this case as in phase radiation condition would not be satisfied. An additional radiating edge is thus created in the form of two slots at the center of antenna. By combining the radiating field of higher order mode patch and fundamental mode of slots a simple single layer, low SLL and high directivity antenna is realized.

3. Theoretical E-plane Radiation Pattern

Theoretical radiation pattern of slot loaded patch antenna can be calculated by using superposition principle. The total far-field is given by the linear combination of patch and slot fields.

$$E_T = E_{Patch} + E_{Slot}. \tag{1}$$

The equivalent aperture model of the antenna is shown in Fig. 3. Here slot 1 and 2 correspond to the effective radiating aperture of TM_{30} mode patch [15] with resonant length along x-axis and represent the patch field, while slot 3 and 4 are radiating aperture corresponding to the resonant slots of about half lambda located at the center of the patch and represent the slot field.

Assuming infinite ground plane, the E-plane ($\phi = 0$) radiated field of TM_{30} mode patch (slot 1 and slot 2) can be calculated [16] and is given as

$$E_{\theta}^{\text{Patch}} = C_1 \cos\left(\frac{3k_0 L}{2}\cos\theta\right),$$
$$C_1 = -\mathrm{j}\frac{k_0 E_a h W}{\pi}\frac{\exp(-\mathrm{j}k_0 r)}{r}. \quad (2)$$

The radiating field of slot (slot 3 and slot 4) due to two element y-directed slot array may be determined using pattern multiplication. For single resonant slot of about half lambda located at origin, electric field can be modeled as that of TE_{10} mode of rectangular waveguide [17] as shown in Fig. 3. The slot aperture field can be written as

$$E_X = E_a \cos\left(\frac{\pi y}{\ell}\right). \quad (3)$$

The radiated field of single slot can be calculated using equivalence principle and is given by

$$E_{\theta} = \frac{-\mathrm{j}k_0 E_a \ell t}{\pi^2}\frac{\cos\left(\frac{k_0\ell}{\pi}\sin\theta\sin\phi\right)}{1-\left(\frac{k_0\ell}{\pi}\sin\theta\sin\phi\right)^2}\frac{\sin\left(\frac{k_0 t}{2}\sin\theta\cos\phi\right)}{\frac{k_0 t}{2}\sin\theta\cos\phi}\cos\phi. \quad (4)$$

Array factor due to two slots along y-axis at distance d apart is given by

$$AF_{34} = 2\cos\left(\frac{k_0 d}{2}\sin\theta\sin\phi\right). \quad (5)$$

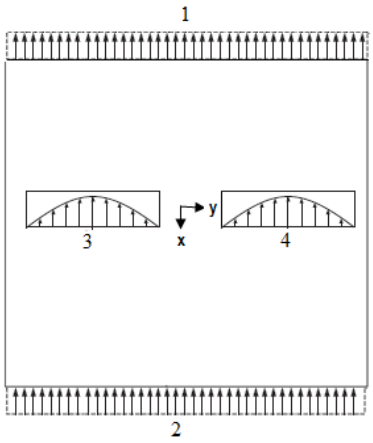

Fig. 3. Equivalent aperture model of the proposed antenna.

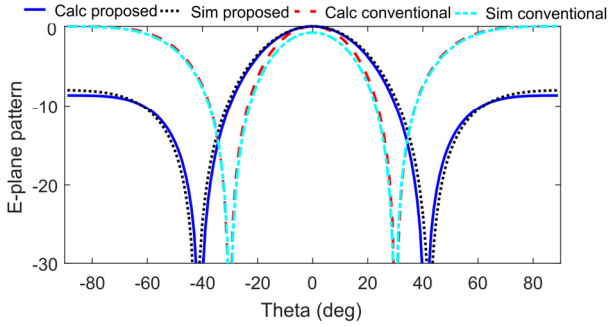

Fig. 4. Simulated and calculated E-plane radiation patterns with infinite ground plane.

Using pattern multiplication the radiated field of slot (slot 3 and slot 4) can be written as

$$E_{\theta}^{\text{slot}} = C_2\frac{\cos\left(\frac{k_0\ell}{\pi}\sin\theta\sin\phi\right)}{1-\left(\frac{k_0\ell}{\pi}\sin\theta\sin\phi\right)^2}\frac{\sin\left(\frac{k_0 t}{2}\sin\theta\cos\phi\right)}{\frac{k_0 t}{2}\sin\theta\cos\phi}\cos\phi\cdot AF_{34},$$
$$C_2 = \frac{-\mathrm{j}2k_0 E_a \ell t}{\pi^2}\frac{\exp(-\mathrm{j}k_0 r)}{r}. \quad (6)$$

For $t << \lambda$ sinc function is approximately equal to 1 and we can write E-plane ($\phi = 0$) pattern as

$$E_{\theta}^{\text{slot}} = C_2. \quad (7)$$

Using (1) the radiated field of slot loaded patch becomes

$$E_{\theta}^{\text{T}} = C_1\cos\left(\frac{3k_0 L}{2}\cos\theta\right) + C_2. \quad (8)$$

Using the optimized slot loaded patch antenna dimensions given in Fig. 2, the far-field amplitude ratio was evaluated and is given by $C_2/C_1 = 0.46$. Figure 4 shows the theoretical and simulated E-plane radiation patterns of the proposed antenna. The simulation was performed in HFSS using infinite ground plane. Both simulated and calculated patterns are in good agreement thus validating the theoretical model. For reference theoretical E-plane radiation pattern of conventional (without slots) TM_{30} mode antenna is also shown in Fig. 4. The reduction in SLL compared to conventional TM_{30} mode patch antenna can be observed from the plot.

4. Parametric Study

The effect of various parameters on the performance of the proposed slot loaded patch antenna has been investigated in this section. Commercial EM simulator Ansys HFSS was used for this parametric study. A finite ground plane 14 cm × 15 cm has been used, and all the simulations were performed in single fed configuration by changing only one parameter at a time while keeping all other parameters constant. The initial parameters of the antenna were $L = 9$ cm, $W = 10$ cm, $\ell = 2.9$ cm, $t = 0.21$ cm, $d = 6$ cm and $F = 1.5$ cm (defined from patch center for single fed configuration).

Simulated S_{11} and directivity plot of the proposed antenna is shown in Fig. 5a and Fig. 5b respectively, ($W = 10$ cm). Two resonance peaks can be observed in the simulated S_{11} curve which corresponds to resonance frequency of the patch and slot respectively (see Sec. 4.2). Moreover, it can be seen from the directivity plot that although the antenna exhibits peak directivity of 12.97 dB at the first resonance frequency of 2.915 GHz but directivity flatness is poor as directivity falls very sharply with frequency reaching a value of –3 dB at 3 GHz. In addition, impedance

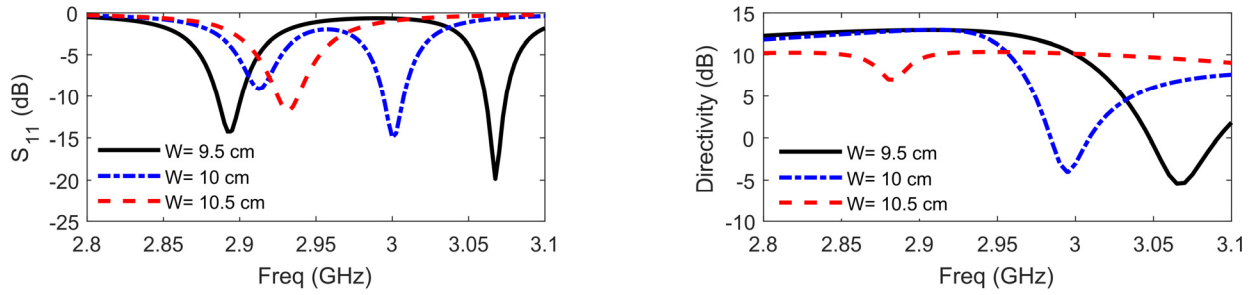

Fig. 5. Effect of patch width W on the proposed slot loaded patch antenna (a) S_{11} and (b) directivity.

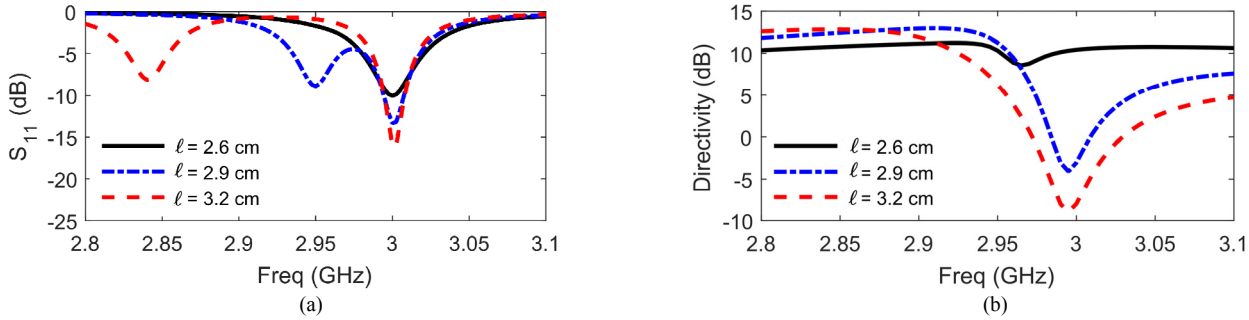

Fig. 6. Effect of slot width ℓ on the proposed slot loaded patch antenna (a) S_{11} and (b) directivity.

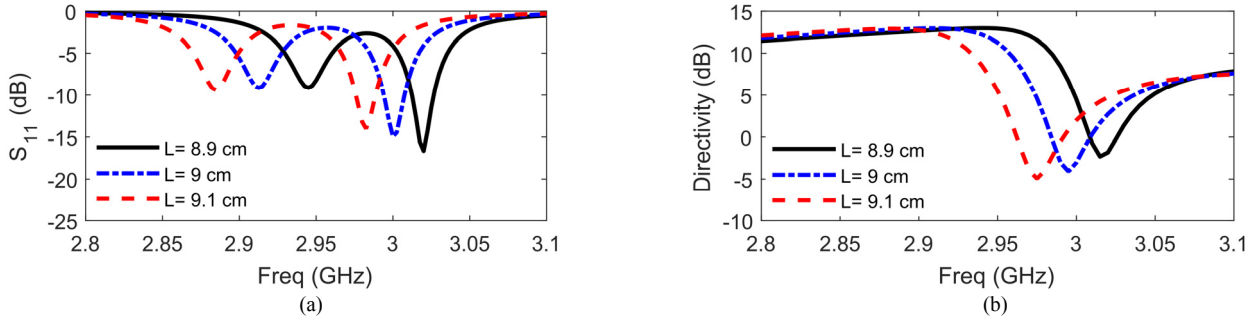

Fig. 7. Effect of patch length L on the proposed slot loaded patch antenna (a) S_{11} and (b) directivity.

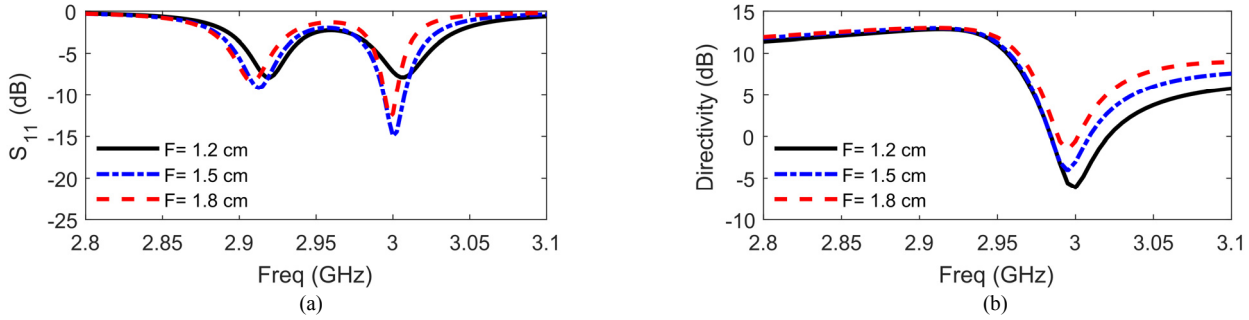

Fig. 8. Effect of feed point position F (non resonant slots, ℓ = 2.9 cm) on the proposed slot loaded patch antenna (a) S_{11} and (b) directivity.

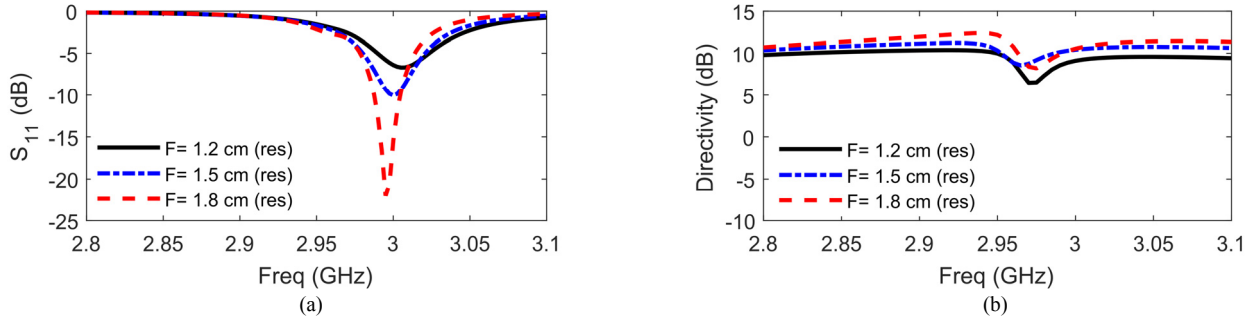

Fig. 9. Effect of feed point position F (resonant slots, ℓ = 2.6 cm) on the proposed slot loaded patch antenna (a) S_{11} and (b) directivity.

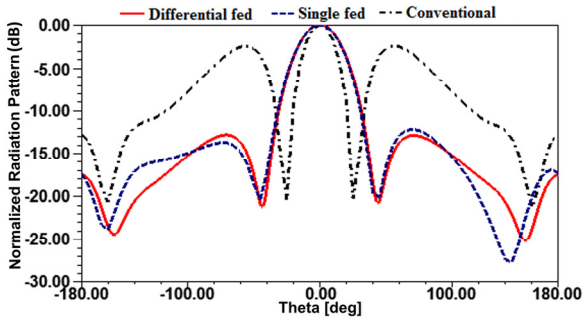

Fig. 10. Comparison of simulated E-plane radiation patterns.

	SLL (E-Plane)	3dB Beamwidth	Directivity	Impedance Bandwidth
Conventional antenna	–2.4 dB	25°	10.9 dB	35 MHz
Single fed antenna	–13.7 dB(L) –12 dB(R)	36°	12.1 dB	20 MHz
Proposed antenna	–12.7 dB	36°	13.3 dB	21 MHz

Tab. 1. Comparison of the proposed, the single fed and the conventional antenna.

matching is also poor at the first resonance peak where directivity is high. Impedance matching cannot be improved by just changing the feed point location. It is shown in Sec. 4.5 that by bringing these two resonance peaks together first and then changing the feed point location good impedance matching can be achieved.

4.1 Effect of Patch Width *W*

It can be seen from Fig. 5a that with increase in W upper resonance peak moves downward while lower resonance peak moves upward. For $W = 10.5$ cm, both peaks merge together at $f = 2.935$ GHz with slightly better impedance matching. Moreover, Figure 5b shows that with increase in W directivity flatness improves significantly. For $W = 10.5$ cm good directivity flatness is achieved but at the expense of reduction in peak directivity.

4.2 Effect of Slot Length ℓ

The slot length ℓ mainly influences the lower resonance peak of the S_{11} curve which corresponds to resonance frequency of slot. It is evident from Fig. 6a that lower resonance peak moves upward as ℓ decreases. The upper resonance frequency (patch resonance) is not influenced by changing slot length. For $\ell = 2.6$ cm, both peaks merge together at $f = 3$ GHz. By combining the two resonance peak together directivity flatness improves greatly as shown in Fig. 6b. For $\ell = 2.6$ cm, good directivity flatness is achieved but at the expense of reduction in peak directivity.

4.3 Effect of Patch Length *L*

Effect of patch length L on S_{11} is shown in Fig. 7a. By increasing length L both resonance peaks move downward. This makes sense as L corresponds to resonant length of the patch antenna and increase in resonant length should result in decrease in resonance frequency. A similar effect can be observed in directivity curve shown in Fig. 7b which also shifts downward with increase in L.

4.4 Effect of Slot Width *t* and Slot Spacing *d*

No significant change in S_{11} and directivity was observed for small variation of slot width t and inter slot spacing d from the nominal values. However, their behavior is similar to that of slot length ℓ and lower resonance peak moves slightly upward as t or d decreases. Moreover, no significant change in directivity flatness was observed for both parameters due to slight change in resonance frequency. Nevertheless, directivity flatness improves slightly with decrease in either slot width t or inter slot spacing d.

4.5 Effect of Feed Point Location *F*

The effect of feed point location F on the S_{11} is shown in Fig. 8a and Fig. 9a. As mentioned previously, the feed point location is defined from patch center for single fed configuration. Two cases are considered, namely resonant slot loading and non resonant slot loading. For resonant slots, slot length $\ell = 2.6$ cm whereas for non resonant slots, slot length $\ell = 2.9$ cm (same as the nominal value). It can be observed from Fig. 8a that S_{11} curve has two resonance peaks for non resonant slots. By varying the feed location F from the nominal value $F = 1.5$ cm, S_{11} at both peaks degrades. Thus no improvement in S_{11} can be achieved by changing the feed point location for non resonant slots. In contrary, for resonant slots varying the feed point location significantly improves the S_{11} and it can be observed from Fig. 9a that by changing the feed point F from 1.5 cm to 1.8 cm, the value of S_{11} decreases from –10 dB to –22 dB. Thus feed point location F improves the impedance matching only for resonant slots.

The effect of feed point location F on the directivity is shown in Fig. 8b and Fig. 9b. In general, directivity flatness for resonant slots is much better compared to non resonant slots. Moreover, it can be observed that directivity flatness is also affected by change in feed location for both cases. This is due to modification of surface current distribution of patch with change in feed point location. The change in surface current also affects the pattern symmetry and cross polarization levels. Thus if a single fed antenna is desired, feed position can be changed to achieve good matching but at the expense of asymmetric radiation pattern and directivity flatness. A differential feeding scheme can be employed to overcome these issues. It is shown in Sec. 5 that differential feeding scheme can be used to achieve symmetric radiation pattern, better directivity flatness and higher directivity compared to single fed design.

Based on the parametric study a slot loaded differential fed patch antenna was optimized. The optimized antenna dimensions are shown in Fig. 2.

5. Comparison of Conventional and Proposed Antenna

In this section comparison of the proposed differential fed slot loaded patch antenna has been carried out with conventional (without slot) higher order TM_{30} mode patch antenna. Commercial EM simulator Ansys HFSS was used for all the simulations. Figure 10 shows the simulated E-plane radiation patterns for the proposed differential fed antenna along with single fed antenna and conventional TM_{30} mode patch antenna.

Significant reduction of SLL compared to conventional TM_{30} mode patch can be observed. The simulated E-plane SLL for TM_{30} mode patch antenna are –2.4 dB while the proposed differential fed slot loaded patch antenna shows SLL of –12.7 dB. Thus, the proposed slot loaded antenna can achieve SLL improvement of more than 10 dB compared to conventional antenna. Moreover, compared to single fed design, the differential fed antenna has symmetric radiation pattern. In addition, the proposed differential fed antenna is suitable for integration with differential integrated circuits and eliminates the need for separate balun.

As shown in Tab. 1, directivity of the proposed differential fed slot loaded patch antenna is 13.3 dB compared to 10.9 dB for conventional TM_{30} mode patch antenna. An improvement of 2.4 dB in directivity is thus achieved while the area remains the same. Moreover, compared to single fed scheme 1.2 dB enhancement of directivity is achieved using differential feeding because it ensures desired in-phase surface current distribution intact as shown in Fig. 1b. It can be seen from Tab. 1 that the proposed antenna exhibits larger 3dB beamwidth of 36° compared to conventional TM_{30} mode patch which has 3dB beamwidth of 25°. The beam broadening can be attributed to reduction in SLL.

The S_{11} plot of the proposed and conventional TM_{30} mode is shown in Fig. 11. Conventional TM_{30} mode patch antenna has a resonance frequency of 3.3 GHz as indicated by the dash line in Fig. 11. In addition, the second resonance frequency at 3 GHz can also be seen in the graph which corresponds to endfire TM_{22} mode. The resonance frequency of the proposed slot loaded patch antenna is at 3 GHz indicated by the solid line in Fig. 11. Thus, in comparison with TM_{30} mode patch having no slot loading, resonance frequency is shifted downward from 3.3 GHz to 3 GHz.

This can be attributed to the increase in current path length due to presence of slot. Moreover, as given in Tab. 1 slot loaded patch antenna shows reduction in impedance bandwidth compared to conventional antenna. The $S_{11} \leq -10$ dB impedance bandwidth of the proposed antenna is 21 MHz compared to conventional TM_{30} mode patch which has an impedance bandwidth of 35 MHz. This reduction in impedance bandwidth can be attributed to

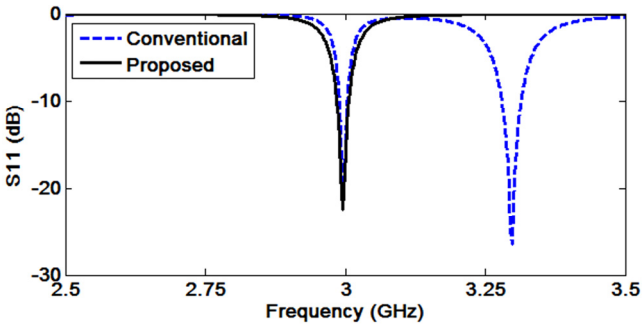

Fig. 11. Simulated S_{11} of the proposed and conventional antenna.

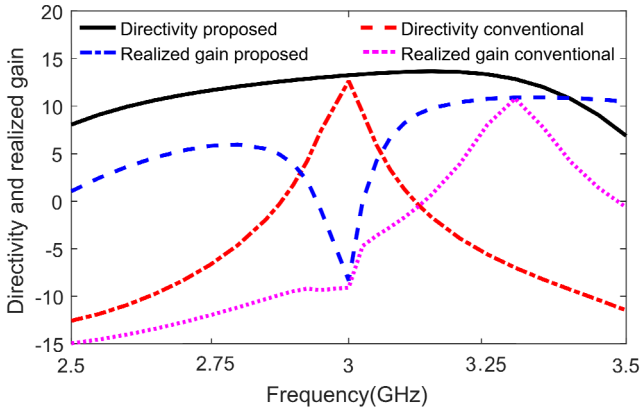

Fig. 12. Simulated directivity and realized gain of the proposed and conventional antenna.

increase in antenna directivity owing to fundamental gain bandwidth product.

The proposed antenna has narrow impedance bandwidth and depending on the actual application, the bandwidth may not be adequate. However, the narrow impedance bandwidth of the proposed antenna can be enhanced by using different techniques like increase in substrate thickness, proximity coupling and stacking. Thus narrow bandwidth of the proposed antenna is not a limitation and can be improved using the aforementioned techniques to meet the actual practical application requirement.

Figure 12 shows the directivity plot of the proposed and conventional antenna as a function of frequency. It is evident from Fig. 12 that the proposed slot loaded antenna has an improved directivity performance. Maximum directivity of the proposed slot loaded antenna is 13.6 dB at 3.15 GHz compared to conventional TM_{30} mode antenna which has maximum directivity of 10.9 dB. Moreover, differential fed slot loaded antenna has better directivity flatness compared to conventional antenna. In fact, for conventional antenna, directivity decreases sharply and reaches a value of –8 dB at 3 GHz. This is due to presence of endfire TM_{22} mode at 3 GHz as shown in Fig. 11. TM_{22} mode is not supported in the proposed differential fed slot loaded antenna as a result it exhibits larger gain bandwidth than the conventional TM_{30} mode patch. Thus in contrary to conventional TM_{30} mode patch antenna, impedance

bandwidth enhancement techniques can be utilized with only slight reduction in antenna directivity.

6. Simulated and Measured Results

In order to validate the performance of the proposed slot loaded patch antenna, a prototype was fabricated. Photograph of the fabricated antenna is shown in Fig. 13. The antenna was differentially fed by using 180° Wilkinson divider shown in Fig. 14. A meander line was utilized in one of the output ports to achieve the desired 180° phase shift. Agilent PNA Network Analyzer was used to measure the reflection coefficient. The simulated and measured S_{11} of the proposed antenna are shown in Fig. 15. The measured $S_{11} \leq -10$ dB impedance bandwidth is 19 MHz compared to simulated S_{11} which was 21 MHz. A slight shift in resonance frequency can be seen in the measured results which may be due to fabrication tolerances.

Figure 16 and 17 show the simulated and measured normalized co-polarization and cross-polarization E and H-planes radiation patterns of the proposed antenna. A compact antenna test range (CATR) was used to measure the far-field radiation patterns of the antenna. The measured antenna gain is 12.8 dBi at 3 GHz. The measured SLL of the antenna is –12 dB and –21.5 dB in E and H-planes respectively. Moreover, the proposed antenna shows a measured cross-polarization level of less than 28.5 dB below co-polarization pattern in both E and H-planes.

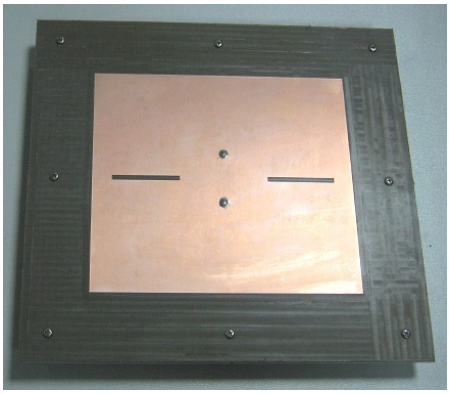

Fig. 13. Prototype of the fabricated differential fed slot loaded TM_{30} mode patch antenna.

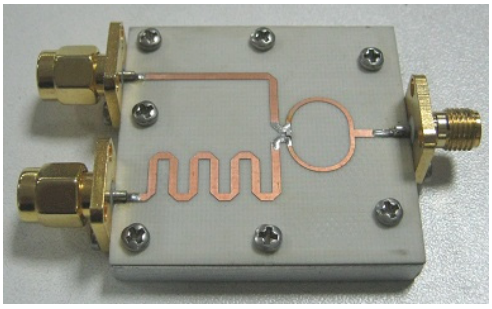

Fig. 14. Fabricated 180° Wilkinson divider used for differential feeding.

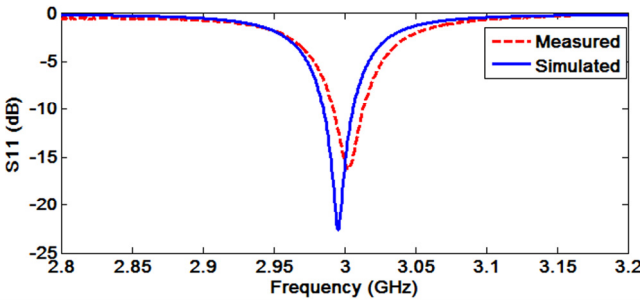

Fig. 15. Simulated and measured S_{11} of the proposed differential fed slot loaded patch antenna.

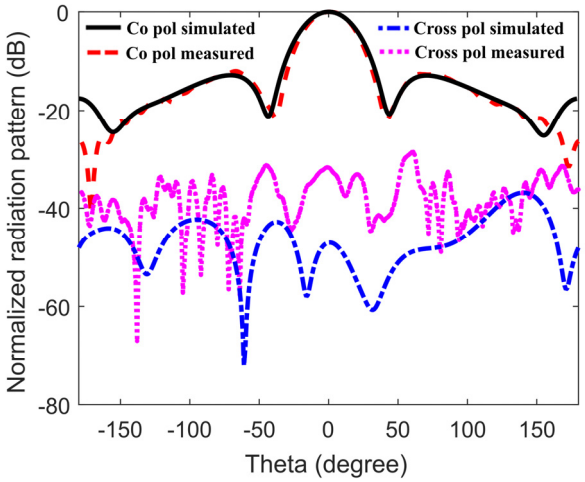

Fig. 16. Simulated and measured E-plane radiation patterns of the proposed differential fed patch antenna.

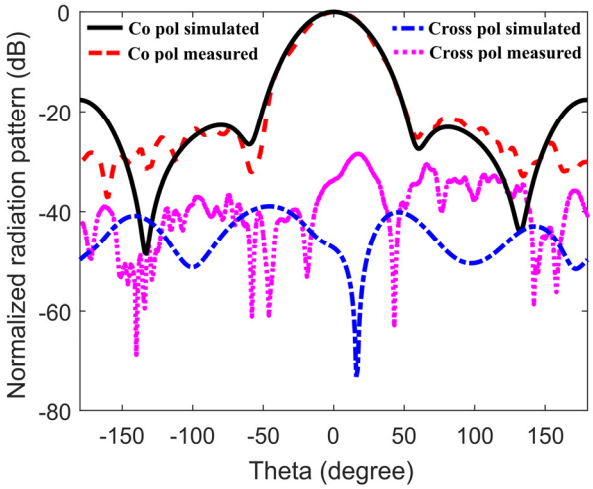

Fig. 17. Simulated and measured H-plane radiation patterns of the proposed differential fed patch antenna.

Reference	Frequency [GHz]	Height	% BW	Directivity [dB]	SLL [dB]
[3]	60	0.025λ	18	10	-
[4]	10	0.042λ	0.7	10.55	–12.1
[6]	10	0.026λ	1.56	10.9	–20
[13]	3.5	0.09λ	12	12.7	–4
Proposed	3	0.015λ	0.7	13.3	–12.7

Tab. 2. Comparison of different single layer high gain patch antennas.

Over the years different techniques have been proposed to enhance the directivity of patch antennas. Multilayer techniques such as stacked patches [18], [19] and use of dielectric [20], [21] or partially reflective superstrate [22], [23] increase the radiating aperture by increasing the volume of the antenna. However, these configurations suffer from geometrical complexity and difficulty to fabricate. Single layer techniques primarily increase the radiating aperture by increasing the surface area of the antenna. Table 2 shows a comparison of different high gain single layer patch antennas found in literature. The proposed antenna demonstrates a high directivity of 13.3 dB using simple Euclidian geometry, previously achieved using Fractal geometries [13]. To the best of our knowledge this is the highest reported peak directivity for TM_{30} mode patch antenna in single layer configuration.

7. Conclusion

High E-plane SLL and low directivity problem of higher order TM_{30} mode patch antenna is resolved by employing resonant slot loading technique and differential feeding. The basic idea of this scheme is to achieve superposition of radiated fields in single layer configuration. This is achieved practically by placing in phase slot radiators, operating in fundamental mode, in the out of phase current distribution region of TM_{30} mode patch antenna. A novel low profile, single layer high gain patch antenna having dimensions of $0.9\lambda_0 \times 1\lambda_0 \times 0.015\lambda_0$ is demonstrated. The proposed differential fed slot loaded higher order mode patch antenna exhibits a 2.4 dB increase in directivity and a reduction of about 10 dB in SLL compared to conventional TM_{30} mode patch antenna. The proposed technique can be utilized to improve the radiation characteristics of higher order mode rectangular patch antennas operating in TM_{m0} (m = 3,5,..) mode.

References

[1] NISHIYAMA, E., AIKAWA, M., EGASHIRA, S. Stacked microstrip antenna for wideband and high gain. *IEE Proceedings-Microwaves, Antennas and Propagation*, 2004, vol. 151, no. 2, p. 143–148. DOI: 10.1049/ip-map: 20040171

[2] JUYAL, P., SHAFAI, L. A high gain single feed dual mode microstrip disc radiator. *IEEE Transactions on Antennas and Propagation*, 2016, vol. 64, no. 6, p. 2115–2126. DOI: 10.1109/TAP.2016.2543804

[3] WANG, D., NG, K. B., CHAN, C. H., WONG, H. A novel wideband differentially-fed higher-order mode millimeter-wave patch antenna. *IEEE Transactions on Antennas and Propagation*, 2015, vol. 63, no. 2, p. 466–473. DOI: 10.1109/TAP.2014.2378263

[4] JUYAL, P., SHAFAI, L. A novel high-gain printed antenna configuration based on TM_{12} mode of circular disc. *IEEE Transactions on Antennas and Propagation*, 2016, vol. 64, no. 2, p. 790–796. DOI: 10.1109/TAP.2015.2506724

[5] KHAN, Q. U, IHSAN, M. B., FAZAL, D., et al. Higher order modes: a solution for high gain, wide band patch antennas for different vehicular applications, *IEEE Transactions on Vehicular Technology*, 2017, vol. 66, no. 5, p. 3548–3554. DOI: 10.1109/TVT.2016.2604004

[6] JUYAL, P., SHAFAI, L. Sidelobe reduction of TM_{12} mode of circular patch via nonresonant narrow slot. *IEEE Transactions on Antennas and Propagation*, 2016, vol. 64, no. 8, p. 3361–3369. DOI: 10.1109/TAP.2016.2576503

[7] LEE, K. F., LUK, K. M., TONG, K. F., et al. Experimental and simulation studies of the coaxially fed U-slot rectangular patch antenna. *IEE Proceedings - Microwave, Antennas and Propagation*, 1997, vol. 144, no. 5, p. 354–358. DOI: 10.1049/ip-map:19971334

[8] YANG, F., ZHANG, X. Z., SAMII, Y. R. Wideband E-shaped patch antennas for wireless communications. *IEEE Transactions on Antennas and Propagation*, 2001, vol. 49, no. 7, p. 1094–1100. DOI: 10.1109/8.933489

[9] KOSSIAVAS, G., PAPIERNIK, A., BOISSET, J. P., et al. The C-patch: a small microstrip element. *Electronics Letters*, 1989, vol. 25, no. 4, p. 253–254. DOI: 10.1049/el:19890177

[10] BHARDWAJ, S., SAMII, Y. R. A comparative study of C-shaped, E-shaped, and U-slotted patch antennas. *Microwave and Optical Technology Letters*, 2012, vol. 54, no. 7, p. 1746–1757. DOI: 10.1002/mop.26894

[11] MACI, S., GENTILI, G. B., AVITABILE, G. Single layer dual frequency patch antenna. *Electronics Letters,* 1993, vol. 29, no. 16, p. 1441–1443. DOI: 10.1049/el:19930965

[12] WATERHOUSE, R. B. Small printed antennas with low cross-polarized fields. *Electronics Letters*, 1997, vol. 33, no. 15, p. 1280–1281. DOI: 10.1049/el:19970873

[13] BORJA, C., FONT, G., BLANCH, S., et al. High directivity fractal boundary microstrip patch antenna. *Electronics Letters*, 2000, vol. 36, no. 9, p. 778–779. DOI: 10.1049/el:20000625

[14] ELLIOTT, R. S. *Antenna Theory and Design*. Hoboken, NJ: John Wiley-IEEE Press, 2003. ISBN: 978-0-471-44996-6

[15] HAMMER, P., VAN BOUCHAUTE, D., VERSCHRAEVEN, D., et al. A model for calculating the radiation field of microstrip antennas. *IEEE Transactions on Antennas and Propagation*, 1979, vol. 27, no. 2, p. 267–270. DOI: 10.1109/TAP.1979.1142054

[16] STUTZMAN, W. L., THIELE, G. A. *Antenna Theory and Design*. 3rd ed. John Wiley & Sons, 2012. ISBN: 978-0-470-57664-9

[17] COLLIN, R. E., ZUCKER, F. J. *Antenna Theory*. New York: McGraw Hill, 1969. ISBN: 978-0070117990

[18] LEE, R. Q., LEE, K. F. Experimental study of the two-layer electromagnetically coupled rectangular patch antenna. *IEEE Transactions on Antennas and Propagation*, 1990, vol. 38, no. 8, p. 1298–1302. DOI: 10.1109/8.56971

[19] EGASHIRA, S., NISHIYAMA, E. Stacked microstrip antenna with wideband and high-gain. *IEEE Transactions on Antennas and Propagation*, 1996, vol. 44, no. 11, p. 1533–1534. DOI: 10.1109/8.542079

[20] JACKSON, D., ALEXOPOULOS, N. Gain enhancement methods for printed circuit antennas. *IEEE Transactions on Antennas and Propagation*, 1985, vol. 33, no. 9, p. 976–987. DOI: 10.1109/TAP.1985.1143709

[21] YANG, H. Y., ALEXOPOULOUS, N. G. Gain enhancement methods for printed circuit antennas through multiple superstrates. *IEEE Transactions on Antennas and Propagation*, 1987, vol. 35, no. 7, p. 860–863. DOI: 10.1109/TAP.1987.1144186

[22] FERESIDIS, A. P., GOUSSETIS, G., WANG, S. H., et al. Artificial magnetic conductor surfaces and their application to low-profile high-gain planar antennas. *IEEE Transactions on Antennas*

and Propagation, 2005, vol. 53, no. 1, p. 209–215. DOI: 10.1109/TAP.2004.840528

[23] FOROOZESH. A., SHAFAI, L. Investigation into effects of the highly reflective patch-type FSS superstrate on the high-gain cavity resonance antenna. *IEEE Transactions on Antennas and Propagation*, 2010, vol. 58, no. 2, p. 258–270. DOI: 10.1109/TAP.2009.2037702

About the Authors ...

Zubair AHMED received the B.Sc. and M.Sc. degrees in Electrical Engineering from the National University of Sciences and Technology (NUST), Islamabad, Pakistan, in 2003, and 2008, respectively. He is currently pursuing his PhD degree at the Department of Electrical Engineering, Capital University of Science and Technology (CUST), Islamabad, Pakistan. His current research interest includes high gain and multiband patch antennas, CRLH TL based metamaterial antennas, microwave filters and integrated RF front ends.

Muhammad Mansoor AHMED completed the PhD degree in Microelectronics from the University of Cambridge, U.K., in 1995, and joined academia where he worked at different positions including Professor; Chairman; Dean and Executive Vice President. He is currently working as Vice Chancellor Capital University of Science and Technology (CUST), Islamabad. Dr. Ahmed research interests are in microelectronics, microwave and RF engineering and he has supervised numerous MS and PhD research projects. He authored over 100 research papers in the field of microelectronics. Dr. Ahmed is a fellow of the Institution of Engineering and Technology (IET), UK.; a Chartered Engineer (CEng) from the UK Engineering Council and holds the title of European Engineer (Eur Ing) from the European Federation of National Engineering Association (FEANI), Brussels. He is a life member of PEC (Pak); EDS & MTTS (USA).

Mojeeb Bin IHSAN received the B.Sc. degree in Electrical Engineering from the University of Engineering and Technology, Lahore, Pakistan, in 1984 and the M.Sc. and Ph.D. degrees in Electrical Engineering from Drexel University, Philadelphia, PA, USA, in 1988 and 1993, respectively. In 1995, he joined the Dept. of Electrical Engineering, College of Electrical and Mechanical Engineering, National University of Sciences and Technology (NUST), Islamabad, Pakistan, where he has established the Microwave Engineering Research Laboratory (MERL) to conduct research and development in electronic systems, development of microwave and radar technology for biomedical applications, microwave active and passive circuits, antennas, radar signal processing, and target classification. He was the Head of the Department of Electrical Engineering, NUST, where he is currently a Professor, as well as acting as the Director of MERL. His current research interests include solid-state electronics, thin-film processing, microwave devices and circuits, and antennas.